Mon. Not. R. Astron. Soc. **369,** 197–206 (2006) doi:10.1111/j.1365-2966.2006.10280.x

Gamma-ray burst efficiency and possible physical processes shaping the early afterglow

Yizhong Fan[1,2,3]★† and Tsvi Piran[1]★

[1]*The Racah Institute of Physics, Hebrew University, Jerusalem 91904, Israel*
[2]*Purple Mountain Observatory, Chinese Academy of Science, Nanjing 210008, China*
[3]*National Astronomical Observatories, Chinese Academy of Sciences, Beijing 100012, China*

Accepted 2006 March 6. Received 2006 March 2; in original form 2006 January 4

ABSTRACT

The discovery by *Swift* that a good fraction of gamma-ray bursts (GRBs) have a slowly decaying X-ray afterglow phase led to the suggestion that energy injection into the blast wave takes place several hundred seconds after the burst. This implies that right after the burst the kinetic energy of the blast wave was very low and in turn the efficiency of production of γ-rays during the burst was extremely high, rendering the internal shocks model unlikely. We re-examine the estimates of kinetic energy in GRB afterglows and show that the efficiency of converting the kinetic energy into γ-rays is moderate and does not challenge the standard internal shock model. We also examine several models, including in particular energy injection, suggested to interpret this slow decay phase. We show that with proper parameters, all these models give rise to a slow decline lasting several hours. However, even those models that fit all X-ray observations, and in particular the energy injection model, cannot account self-consistently for both the X-ray and the optical afterglows of well-monitored GRBs such as GRB 050319 and GRB 050401. We speculate about a possible alternative resolution of this puzzle.

Key words: radiation mechanisms: non-thermal – ISM: jets and outflows – gamma-rays: bursts – X-rays: general.

1 INTRODUCTION

The X-ray telescope (XRT) onboard *Swift* has provided high-quality early X-ray afterglow light curves of many gamma-ray bursts (GRBs). One of the most remarkable and unexpected features discovered by *Swift* was that many of these X-ray afterglow light curves are distinguished by a slow decline – the flux F decreases with observer's time t as $F \propto t^{[0,-0.8]}$, lasting from a few hundred seconds to few hours (Campana et al. 2005; Cusumano et al. 2006; Nousek et al. 2005; Vaughan et al. 2006; de Pasquale et al. 2006). Such a phase is unexpected in the standard fireball model. A simple explanation is that the slow decline arises due to a significant energy injection (Nousek et al. 2005; Zhang et al. 2005; Granot & Kumar 2006; Panaitescu et al. 2006), as suggested previously (for baryon-rich injection, see Panaitescu, Mészáros & Rees 1998; Rees & Mészáros 1998; Kumar & Piran 2000; Sari & Mészáros 2000; Zhang & Mészáros 2002; Granot, Nakar & Piran 2003; for Poynting flux-dominated injection[1], see Dai & Lu 1998a; Zhang & Mészáros 2001; Dai 2004. It has been argued that consequently the resulted GRB efficiency, i.e. the ratio of the energy emitted in γ-ray energy to the total energy (the sum of the γ-ray energy and the kinetic energy of the ejecta powering the afterglow), should be 90 per cent or higher. Some extreme assumptions are needed (Beloborodov 2000; Kobayashi & Sari 2001) to reach such a high efficiency within the framework of the standard internal shocks model (Paczynski & Xu 1994; Rees & Mészáros 1994; Kobayashi, Piran & Sari 1997; Sari & Piran 1997a,b; Daigne & Mochkovitch 1998; Piran 1999).

We re-examine this issue focusing on two critical aspects of the analysis. The estimate of the kinetic energy of the ejecta from the afterglow observations and in particular from the X-ray flux and the need of energy injection. We show in Section 2 that even for these *Swift* GRBs with long duration X-ray flattening the γ-ray conversion efficiency is high but not unreasonable.

We then turn to the puzzling slow decline seen in the first few hours of the X-ray afterglow. We explore in Section 3 several models that may give rise to slowly decaying X-ray afterglows. (i) Energy injection. (ii) A small ζ_e, in which only a small fraction, $\zeta_e \ll 1$

★E-mail: yzfan@pmo.ac.cn (YF); tsvi@phys.huji.ac.il (TP)
†Lady Davis Fellow.

[1] If the outflow ejected from the central engine after the GRB phase is highly magnetized, at a radius $\sim 10^{15}$ cm, the magnetohydrodynamics (MHD) condition breaks down. Significant magnetic field dissipation processes are expected to happen which converts energy into radiation. As long as the highly magnetized outflow is steady enough, strong and slowly decaying X-ray emission is possible (see Fan, Zhang & Proga 2005a and the references therein).

of the electrons are accelerated to high energies and contribute to the radiation process. (iii) Evolving shock parameters, where the microscopic shock parameters ϵ_e and/or ϵ_B (the fraction of shock energy given to the magnetic filed) vary in time and are inversely proportional to the Lorentz factor of the ejecta. (iv) A very low-variable external density model, in which the number density of the medium is not only very low but it also a function of the radius. (v) Highly magnetized outflow where flattening might arise because of a slow conversion of the magnetic energy to kinetic energy of the external matter. We present in Section 3 analytical derivation as well as numerical calculations of the expected light curves in all these models except the last one. In Section 4, we compare the models to the observations of GRB 050319 and GRB 050401. We summarize our results and discuss their implications in Section 5. We conclude with a speculation on the nature of the solution to this puzzle.

2 IS THERE A GRB EFFICIENCY CRISIS?

One of the critical factors that characterize the emitting of a GRB is the energy conversion efficiency. The γ-ray efficiency is defined as

$$\epsilon_\gamma \equiv \frac{E_\gamma}{E_\gamma + E_k}, \tag{1}$$

where E_γ is the isotropic equivalent energy of the γ-ray emission and E_k is the isotropic equivalent energy of the outflow powering the afterglow. Following the *Swift* observations of flattening in the X-ray afterglow light curve of many GRBs, it has been argued that typical values of ϵ_γ could be as high as 90 per cent or even higher (Ioka et al. 2005; Nousek et al. 2005; Zhang et al. 2005; for the discussion of pre-*Swift* GRBs, see Llod-Ronning & Zhang 2004, hereafter LZ04). This very high efficiency would challenge most γ-ray emission models and in particular it challenges the standard fireball model that is based on internal shocks.

These claims arise from revised estimates of the kinetic energy immediately following the GRB. Therefore, in order to explore this issue we re-examine the estimates of the kinetic energy from the X-ray observations. As we show below, at a late afterglow epoch, the X-ray band is above the cooling frequency. In this case, the X-ray flux is independent of the poorly constrained n and the X-ray luminosity is a good probe of E_k (Kumar 2000; Freedman & Waxman 2001, LZ04).

In the standard GRB afterglow model (e.g. Sari, Piran & Narayan 1998; Piran 1999), the X-ray afterglow is produced by a shock propagating into the circumburst matter. The equations that govern the emission of this shock are (Yost et al. 2003)[2]

$$F_{\nu,\max} = 6.6\,\mathrm{mJy}\left(\frac{1+z}{2}\right) D_{\mathrm{L},28.34}^{-2}\epsilon_{B,-2}^{1/2}E_{k,53}n_0^{1/2}, \tag{2}$$

$$\nu_\mathrm{m} = 7.6\times10^{11}\,\mathrm{Hz}\,E_{k,53}^{1/2}\epsilon_{B,-2}^{1/2}\epsilon_{\mathrm{e},-1}^{2}C_p^2\left(\frac{1+z}{2}\right)^{1/2} t_\mathrm{d}^{-3/2}, \tag{3}$$

$$\nu_\mathrm{c} = 1.4\times10^{15}\,\mathrm{Hz}\,E_{k,53}^{-1/2}\epsilon_{B,-2}^{-3/2}n_0^{-1}\left(\frac{1+z}{2}\right)^{-1/2} t_\mathrm{d}^{-1/2}\frac{1}{(1+Y)^2}, \tag{4}$$

where z is the redshift, D_L is the corresponding luminosity distance, p is the power-law index of the shocked electrons, we use $p = 2.3$ throughout this work, $C_p \equiv 13(p-2)/[3(p-1)]$ and t_d is the observer's time in unit of days. $Y = (-1+\sqrt{1+4\eta\eta_\mathrm{KN}\epsilon_\mathrm{e}/\epsilon_B})/2$ is the Compton parameter, where $\eta = \min\{1, (\nu_\mathrm{m}/\nu_\mathrm{c})^{(p-2)/2}\}$ (e.g. Sari, Narayan & Piran 1996; Wei & Lu 1998, 2000), $0 \leqslant \eta_\mathrm{KN} \leqslant 1$ is a coefficient accounting for the Klein–Nishina effect, which is γ_e (the random Lorentz factor of the electron) dependent (see Appendix A for detail). Here and throughout this text, the convention $Q_x = Q/10^x$ has been adopted in CGS units.

For the typical parameters taken here, ν_m crosses the observer frequency $\nu_\mathrm{X} \sim 10^{17}$ Hz at $t_\mathrm{d} \sim 4\times10^{-4}$. It is quite reasonable to assume $\nu_\mathrm{X} > \max\{\nu_\mathrm{c}, \nu_\mathrm{m}\}$, and the predicted X-ray flux is

$$\begin{aligned} F_{\nu_\mathrm{X}} &= F_{\nu,\max}\nu_\mathrm{c}^{1/2}\nu_\mathrm{m}^{(p-1)/2}\nu_\mathrm{X}^{-p/2} \\ &= 3.8\times10^{-4}\,\mathrm{mJy}\left(\frac{1+z}{2}\right)^{(2+p)/4} D_{\mathrm{L},28.34}^{-2}\epsilon_{B,-2}^{(p-2)/4}\epsilon_{\mathrm{e},-1}^{p-1} \\ &\quad\times E_{k,53}^{(p+2)/4}(1+Y)^{-1}t_\mathrm{d}^{(2-3p)/4}\nu_{X,17}^{-p/2}. \end{aligned} \tag{5}$$

The flux recorded by XRT is

$$\begin{aligned} \mathcal{F} &= \int_{\nu_{X1}}^{\nu_{X2}} F_{\nu_\mathrm{X}}\,\mathrm{d}\nu_\mathrm{X} \\ &= 1.2\times10^{-12}\,\mathrm{erg\,s^{-1}\,cm^{-2}}\left(\frac{1+z}{2}\right)^{(p+2)/4} D_{\mathrm{L},28.34}^{-2} \\ &\quad\times\epsilon_{B,-2}^{(p-2)/4}\epsilon_{\mathrm{e},-1}^{p-1}E_{k,53}^{(p+2)/4}(1+Y)^{-1}t_\mathrm{d}^{(2-3p)/4}, \end{aligned} \tag{6}$$

where $\nu_{X1} = 0.2$ keV and $\nu_{X2} = 10$ keV. This equation is now inverted to obtain E_k from the observed flux.

In some special cases, $\nu_\mathrm{m} < \nu_\mathrm{X} < \nu_\mathrm{c}$, the flux recorded by XRT should be

$$\begin{aligned} \mathcal{F} &= 1.5\times10^{-11}\,\mathrm{erg\,s^{-1}\,cm^{-2}}\left(\frac{1+z}{2}\right)^{(p+3)/4} D_{\mathrm{L},28.34}^{-2} \\ &\quad\times\epsilon_{B,-2}^{(p+1)/4}\epsilon_{\mathrm{e},-1}^{p-1}n_0^{1/2}E_{k,53}^{(p+3)/4}t_\mathrm{d}^{3(1-p)/4}, \end{aligned} \tag{7}$$

2.1 The efficiency of the pre-*Swift* GRBs

With equation (6), the corresponding X-ray luminosity at $t_\mathrm{d} = 0.4$ (∼10 h, to compare with the results of LZ04) is

$$\begin{aligned} L_\mathrm{X} &= 4\pi D_\mathrm{L}^2\mathcal{F}/(1+z) \\ &= 1.1\times10^{46}\,\mathrm{erg\,s^{-1}\,cm^{-2}}\left(\frac{1+z}{2}\right)^{(p-2)/4} \\ &\quad\times\epsilon_{B,-2}^{(p-2)/4}\epsilon_{\mathrm{e},-1}^{p-1}(1+Y)^{-1}E_{k,53}^{(p+2)/4}, \end{aligned} \tag{8}$$

[2] To derive these equations, the deceleration of the fireball is governed by the energy conservation $\Gamma^2\,Mc^2 = E_k$, where M is the rest mass of the shocked medium (e.g. Blandford & McKee 1976; Sari et al. 1998; Piran 1999). The distribution of the fresh electrons accelerated by the shock is assumed to be $\mathrm{d}n/\mathrm{d}\gamma_\mathrm{e} \propto \gamma_\mathrm{e}^{-p}$ for $\gamma_\mathrm{e} \geqslant \gamma_\mathrm{e,m}$, where $\gamma_\mathrm{e,m} = (m_\mathrm{p}/m_\mathrm{e})[(p-2)/(p-1)]\epsilon_\mathrm{e}(\Gamma-1)$, governed by the strict shock jump conditions (Blandford & McKee 1976). The other crucial parameter is the cooling Lorentz factor $\gamma_\mathrm{e,c} = 6(1+z)\,\pi m_\mathrm{e}\,c/[\sigma_\mathrm{T}\,\Gamma B^2\,t(1+Y)]$, above which the energy loss due to the synchrotron/inverse Compton radiation is important (Sari et al. 1998; Piran 1999), where σ_T is the Thompson cross-section and B is the magnetic field of the shocked medium. ν_m and ν_c are the corresponding synchrotron radiation frequency of electrons with Lorentz factors $\gamma_\mathrm{e,m}$ and $\gamma_\mathrm{e,c}$, respectively. The maximum specific flux is estimated as $F_{\nu,\max} \approx (1+z)M\Gamma e^3\,B/(4\pi m_\mathrm{p}\,m_\mathrm{e}\,c^2\,D_\mathrm{L}^2)$ (Sari et al. 1998; Wijers & Galama 1999), where e is the charge of electron. The ν_c and F_ν,max taken here are comparable with that of most previous works (e.g. Granot, Piran & Sari 1999; Wijers & Galama 1999; Panaitescu & Kumar 2002; LZ04). The ν_m is close to that taken in Sari et al. (1998), Granot et al. (1999) and Wijers & Galama (1999), but is about 30–40 times smaller than that taken in Panaitescu & Kumar (2002) and LZ04. Such a large divergency may arise if one ignores the term $(p-2)/(p-1)$ when evaluating $\gamma_\mathrm{e,m}$.

Table 1. GRB energies and efficiencies, L_X used in equation (9) and E_γ are all taken from LZ04. The numerical values quoted in parentheses are for $(1+Y) \simeq (\epsilon_e/\epsilon_B)^{1/2}$.

GRB	$E_\gamma/10^{52}$ (erg)	$E_k/10^{52}$ (erg)	Efficiency ϵ_γ
970228	1.42	17.5 (47.5)	0.08 (0.03)
970508	0.55	9.1 (24.8)	0.06 (0.02)
970828	21.98	37.4 (101.5)	0.37 (0.18)
971214	21.05	78.0 (212)	0.21 (0.09)
980613	0.54	11.2 (30.5)	0.05 (0.02)
980703	6.01	22.2 (60.2)	0.21 (0.09)
990123	143.8	186.6 (507)	0.43 (0.22)
990510	17.6	121.1 (329)	0.13 (0.05)
990705	25.6	3.1 (8.5)	0.89 (0.75)
991216	53.5	337.1 (916)	0.14 (0.06)
000216	16.9	4.6 (12.5)	0.78 (0.58)
000926	27.97	91.7 (249.3)	0.23 (0.1)
010222	85.78	209.7 (569.8)	0.29 (0.13)
011211	6.72	12.1 (33)	0.36 (0.17)
020405	7.2	42.3 (115)	0.15 (0.06)
020813	77.5	203.9 (554)	0.28 (0.12)
021004	5.56	76.8 (208.8)	0.07 (0.03)
XRF 020903	0.0011	0.09 (0.25)	0.01 (0.004)

which in turn yields

$$E_k = 9.2\times10^{52}\,\mathrm{erg}\,RL_{X,46}^{4/(p+2)}\left(\frac{1+z}{2}\right)^{(2-p)/(p+2)} \times \epsilon_{B,-2}^{-(p-2)/(p+2)}\epsilon_{e,-1}^{4(1-p)/(p+2)}(1+Y)^{4/(p+2)}, \quad (9)$$

where $R \sim [t(10\,\mathrm{h})/T_{90}]^{17\varepsilon}\mathrm{e}/16$ is a factor accounting for the energy radiative loss during the first 10 h following the prompt γ-ray emission phase (Sari 1997; LZ04), T_{90} is the duration of the GRB. The numerical factor of our equation (9) is larger than that of equation (7) of LZ04 by a factor of $9.2(1+Y)^{4/(p+2)}$ due to the facts that (1) the ν_m taken here, which matches the numerical result better (one can verify this with a simple code to calculate the dynamical evolution as well as ν_m numerically), is about one and half orders smaller than that taken in LZ04. (2) The inverse Compton effect has been taken into account. Similar conclusions have been reached by Granot et al. (2006). However, it is not easy to estimate Y since it depends on ϵ_B sensitively (see Appendix B for discussion). One good way to estimate the GRB efficiency may be to take $Y \sim 0$ and $(1+Y) \sim (\epsilon_e/\epsilon_B)^{1/2}$, respectively. In both cases, our estimates of ϵ_γ (Table 1) are significantly lower than those of LZ04.[3] Smaller ϵ_γ may be possible in view of that both ϵ_e and ϵ_B might be significantly lower than the standard parameters taken here (Panaitescu & Kumar 2002). We suggest that the typical GRB efficiency of these pre-*Swift* bursts is ∼0.1 (see Table 1 for detail). Such values are well understood within the internal shock model.

Additional support for this conclusion arises from late energy estimates. Berger, Kulkarni & Frail (2004) used the late-time radio observation to estimate the kinetic energy at this stage. The find high energies and correspondingly low γ-ray efficiency. For GRB 970508 and GRB 970803, the efficiencies are 0.03 and 0.2, respectively, which coincide with our estimates (see Table 1).

[3] While our results are very close to the recent calculations of Granot et al. (2006), they also show that the estimates of E_k are very sensitive to the exact expressions used for ν_c, ν_m and $F_{\nu,\max}$. Similar conclusion can be drawn by comparing previous results of Granot et al. (1999), Wijers & Galama (1999), Freedman & Waxman (2001), Panaitescu & Kumar (2002) and LZ04. Therefore, an alternative explanation for the apparent high efficiencies is that the blast wave energy estimates using L_X are simply inaccurate.

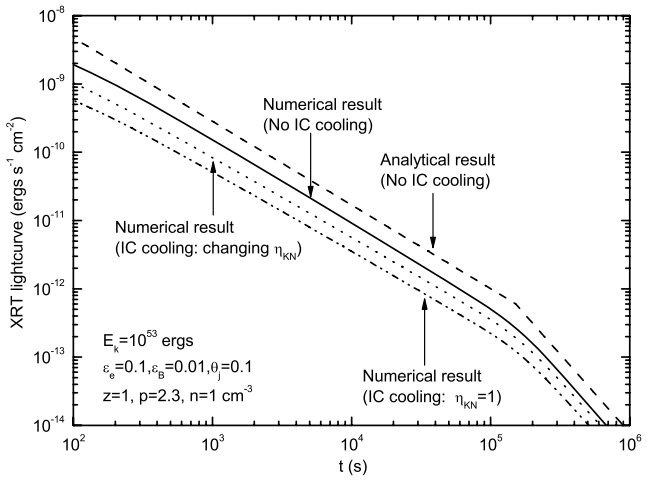

Figure 1. X-ray (0.2–10 keV) afterglow light curves: analytical (dashed line) light curve, and numerical (solid line) when Inverse Compton effect has been ignored. The divergence is about a factor of 2. Numerical estimates when the inverse Compton effect has been taken into account with (dotted line) and without (dashed–dotted line) a Klein–Nishina correction. Clearly, the Klein–Nishina correction is unimportant for the fiducial parameters listed in the figure.

The coefficient of our equation (9) are very different from that of equation (7) of LZ04. Below we check its validity numerically. The code used here has already been used in Zhang et al. (2005) and has been tested by J. Dyks independently (Dyks, Zhang & Fan 2005). Here, we just describe briefly the technical treatment. The dynamical evolution of the outflow is calculated with the formulae presented in Huang et al. (2000), which are able to describe the dynamical evolution of the outflow in both the relativistic and the non-relativistic phases. The electron energy distribution is calculated by solving the continuity equation with the power-law source function $Q = K\gamma_e^{-p}$, normalized by a local injection rate. The cooling of the electrons due to both synchrotron and inverse Compton (Moderski, Sikora & Bulik 2000) has been taken into account.

Fig. 1 depicts the numerical results. One can see that the numerical results match the analytical ones to within a factor of 2. We therefore conclude that equations (6) and (9) are reasonable approximations to the full solution of the problem.

2.2 The GRB efficiency of *Swift* GRBs with X-ray flattening

Early flattening is evident for a good fraction of the X-ray afterglow light curves recorded by the *Swift* XRT. Determination of the GRB efficiency of these GRBs is quite challenging since, as we see in Section 4 the underlying physical process that controls the slow decline is unclear. A common interpretation for this flat decay is energy injection, which essentially increases the required initial GRB efficiency. In spite of the uncertainties concerning the applicability of this model we consider its implication to the efficiency.

The energy injection is characterized by a factor f such that fE_k($f \sim$ a few tens; in the following discussion, we take $f = 5$) is the energy injected into the fireball (Zhang et al. 2005). The initial GRB efficiency should be

$$\tilde{\epsilon}_\gamma \equiv \frac{E_\gamma}{E_\gamma + E_k} = \frac{f\epsilon_\gamma}{1+(f-1)\epsilon_\gamma}, \quad (10)$$

where $\epsilon_\gamma \equiv E_\gamma/(E_\gamma + fE_k)$ is the GRB efficiency derived at $t_d \sim 0.4$. LZ04 find that $\epsilon_\gamma > 0.4$, and therefore, $\tilde{\epsilon}_\gamma > 0.8$, which is too high within the framework of the standard (internal shocks) fireball model. However, as shown in Section 2.1, ϵ_γ presented in LZ04 has been overestimated significantly. We suggest that $\epsilon_\gamma \sim 0.1$, therefore even when correcting for the additional energy $\tilde{\epsilon}_\gamma \sim 0.3$, which is still consistent with this model.

As an example, we consider the γ-ray efficiency of GRB 050319. Both the optical (Mason et al. 2006) and the X-ray (Cusumano et al. 2006) light curves are well recorded for this burst and can be used to constrain the efficiency (see Section 4.1 for a detailed discussion). (1) The time-averaged optical-to-X-ray spectrum ($t \sim 200$–900 s) is a single power law with an index $\beta = -0.8$ (Mason et al. 2006). This implies that $\nu_m(t \sim 100\,\mathrm{s}) < \nu_R = 4.3 \times 10^{14}$ Hz. (2) The very early R-band observation suggests that $F_{\nu,\max}(t \sim 100\,\mathrm{s}) \sim 1$ mJy (assuming that energy injection takes place at $t \geqslant 400$ s). (3) $\nu_c > \nu_X \sim 10^{17}$ Hz holds up to $t \sim 10^6$ s, as suggested by the XRT spectrum. We have (see equations 31–33) $\epsilon_e \sim 4 \times 10^{-2}$, $\epsilon_B \sim 4 \times 10^{-5}$, and $E_k \sim 1.3 \times 10^{54}$ erg (the energy carried by the initial outflow). With K-correction, the isotropic energy of the γ-ray emission of GRB 050319 is $E_\gamma \sim 1.2 \times 10^{53}$ erg (Nousek et al. 2005), so $\tilde{\epsilon}_\gamma = E_\gamma/(E_\gamma + E_k) \sim 0.1$. It is sufficiently low to be well understood within the standard fireball model.

3 MODELS FOR A SLOWLY DECAYING X-RAY AFTERGLOW

We turn now to explore (both analytically and numerically) models that can give rise to a slowly decaying X-ray afterglow phase. The models we discuss include: (i) energy injection; (ii) a small ζ_e; (iii) evolving shock parameters and (iv) a very low non-constant circumburst density. We also examine the possibility of the X-ray flattening is attributed to a highly magnetized outflow. In the numerical calculations that we present the parameters are chosen to reproduce the XRT light curve of GRB 050319 (for $t > 380$ s). We also present the corresponding R-band light curve.

3.1 Energy injection

In the standard fireball model, the fireball that is sweeping the circumburst matter decelerates and its bulk Lorentz factor evolves with the time as $\Gamma \propto t^{-3/8}$. With continuous significant energy injection, the fireball decelerates more slowly and slowly decaying multiwavelength afterglows are expected. This model has been analytically investigated by many authors (Sari & Mészáros 2000; Nousek et al. 2005; Zhang et al. 2005; Granot & Kumar 2006; Panaitescu et al. 2006). As shown in Zhang et al. (2005), for $\mathrm{d}E_{\rm inj}/\mathrm{d}t \propto t^{-q}$ we find $\nu_m \propto t^{-(2+q)/2}$, $\nu_c \propto t^{(q-2)/2}$ and $F_{\nu,\max} \propto t^{1-q}$. In this subsection, we take $q = 0.5$ and find

$$F_\nu \propto \begin{cases} t^{(8-7q)/6} \sim t^{0.75}, & \text{for } \nu < \nu_c < \nu_m; \\ t^{(2-3q)/4} \sim t^{1/8}, & \text{for } \nu_c < \nu < \nu_m; \\ t^{(8-5q)/6} \sim t^{0.92}, & \text{for } \nu_c < \nu < \nu_m; \\ t^{[(6-2p)-(p+3)q]/4} \sim t^{-0.32}, & \text{for } \nu_m < \nu < \nu_c; \\ t^{[(4-2p)-(p+2)q]/4} \sim t^{-0.68}, & \text{for } \nu > \max\{\nu_c, \nu_m\}. \end{cases} \quad (11)$$

Following Zhang et al. (2005), we consider an energy injection rate of the form $(1+z)\,\mathrm{d}E_{\rm inj}/\mathrm{d}t = Ac^2(t/t_0)^{-q}$ for $t_0 < t < t_e$, where A is a constant. With the energy injection, equation (8) of Huang et al. (2000) should be replaced by (see also Wei, Yan & Fan 2006)

$$\mathrm{d}\Gamma = \frac{(1-\Gamma^2)\,\mathrm{d}m + A(t/t_0)^{-q}[\mathrm{d}t/(1+z)]}{M_{\rm ej} + \epsilon m + 2(1-\epsilon)\Gamma m}, \quad (12)$$

where $M_{\rm ej}$ is the rest mass of the initial GRB ejecta, m is the mass of the medium swept by the GRB ejecta, which is governed by $\mathrm{d}m = 4\pi R^2\, nm_p\, \mathrm{d}R$, m_p is the rest mass of proton, $\mathrm{d}R = \Gamma(\Gamma + \sqrt{\Gamma^2 - 1})c\mathrm{d}t/(1+z)$, $\epsilon = \eta\epsilon_e$ is the radiation efficiency. Our numerical results, the R-band emission and the 0.2–10 keV emission, are shown in Fig. 2.

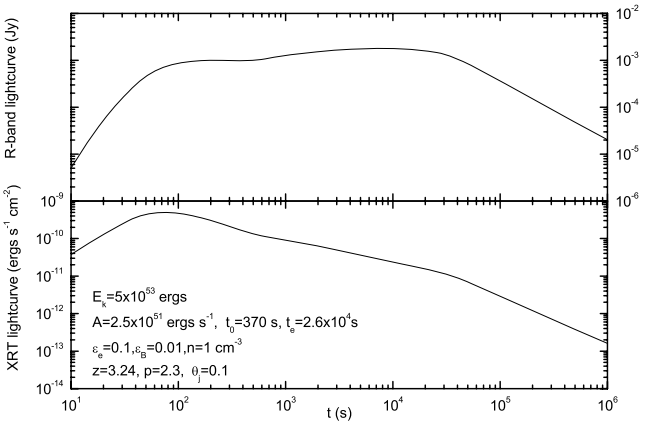

Figure 2. The X-ray (0.2–10 keV) afterglow light curve and the R-band light curve for the energy injection model.

3.2 Small ζ_e

In the standard afterglow model, it is assumed that a fraction ϵ_e of the shock energy is given to all the fresh electrons that are swept by the shock front. However, it is possible that only a fraction ζ_e of fresh electrons has been accelerated, as suggested by Papathanassiou & Mészáros (1996). With this correction, equations (2) and (3) take the form

$$F_{\nu,\max} = 6.6\,\mathrm{mJy}\,\zeta_e \left(\frac{1+z}{2}\right) D_{\mathrm{L},28.34}^{-2} \epsilon_{B,-2}^{1/2} E_{k,53} n_0^{1/2}, \quad (13)$$

$$\nu_m = 7.6 \times 10^{11}\,\mathrm{Hz}\,\zeta_e^{-2} E_{k,53}^{1/2} \epsilon_{B,-2}^{1/2} \epsilon_{e,-1}^2 C_p^2 \left(\frac{1+z}{2}\right)^{1/2} t_d^{-3/2}, \quad (14)$$

respectively.

For $\nu_c < \nu_X < \nu_m$, $F_{\nu_X} \propto t^{-1/4}$. A steeper decline is possible (the steepest one is $F_{\nu_X} \propto t^{-4/7}$), depending on the radiative correction, as shown in the upper panel of fig. 2 of Sari et al. (1998).

The transition of the slow decline to a normal decline ($F_{\nu_X} \propto t^{-1.2}$) usually takes place at $t \sim 0.1$ d or earlier, when $\nu_X = \nu_m$. So we have

$$\zeta_e \simeq 0.016 E_{k,53}^{1/4} \epsilon_{e,-1} \epsilon_{B,-2}^{1/4} t_{d,-1}^{-3/4} C_p \left(\frac{2}{1+z}\right)^{1/2}. \quad (15)$$

The numerical light curve is presented in Fig. 3. One can see that a long-time multiwavelength flattening is evident with a small ζ_e.

Before and after the temporal decline transition, the energy spectrum of the XRT observation should be $F_\nu \propto \nu^{-1/2}$ and $F_\nu \propto \nu^{-p/2}$, respectively. In other words, after the break in the light curve, the X-ray spectrum should be much softer (see also Zhang et al. 2005), which is inconsistent with most XRT observations (Nousek et al.

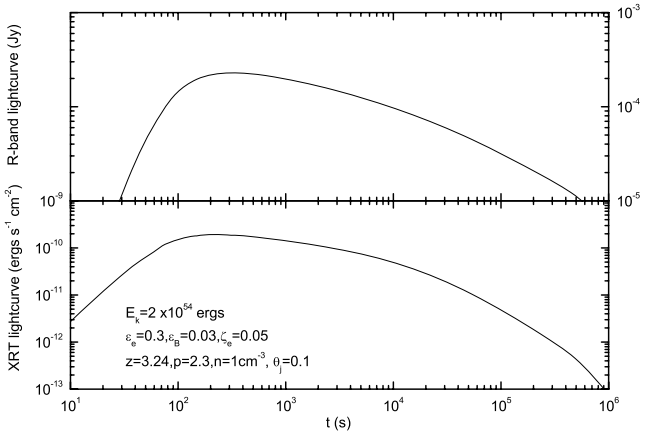

Figure 3. The X-ray (0.2–10 keV) afterglow light curve and the *R*-band light curve for the small ζ_e model.

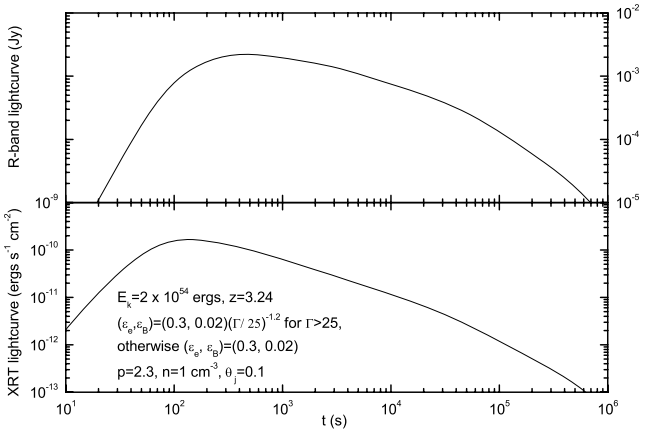

Figure 4. The X-ray (0.2–10 keV) and *R*-band afterglow light curves for the evolving shock parameter model. The parameters are listed in the figure.

2005). In addition, in this model, the spectral index of the XRT afterglows in the slow decline phase is $-1/2$. It is much harder than that of most *Swift* X-ray afterglows (see table 1 of Nousek et al. 2005). The *Swift* observations therefore provide us robust evidences of that significant part of, rather than a small fraction of electrons, have been accelerated in the shock front.

3.3 Evolving shock parameters

In the standard afterglow model, the shock parameters ϵ_e and ϵ_B are assumed to be constant. However, it is also possible that ϵ_e or ϵ_B, or both, vary with time (see Yost et al. 2003, for detailed discussion). Fan et al. (2002) and Wei, Yan & Fan (2006) modelled the optical flares detected in GRB 990123 and GRB 050904 and found that both ϵ_e and ϵ_B of the forward shock (ultrarelativistic) and reverse shock (mild relativistic to relativistic) were very different. This provides an indication evidence for a dependence of the shock parameters on the strength of the shock. Possible evidence for the shock strength-dependent ϵ_B was also found by Zhang, Kobayashi & Mészáros (2003), Kumar & Panaitescu (2003), McMahon, Kumar & Panaitescu (2004), Panaitescu & Kumar (2004), Fan, Zhang & Wei (2005b) and Blustin et al. (2006). Yost et al. (2003) and Ioka et al. (2005) considered afterglow emission assuming ϵ_B and ϵ_e are time-dependent, respectively. Here we simply take $(\epsilon_e, \epsilon_B) \propto (\Gamma^{-a}, \Gamma^{-b})$ for $\Gamma > \Gamma_o$, otherwise $(\epsilon_e, \epsilon_B) \sim$ constant, where Γ_o is the Lorentz factor of the outflow at the X-ray decline translation, both a and b are taken to be positive. For simplicity, we discuss only the case of $a = b$ for $\Gamma > \Gamma_o$. Below Γ_o, the solution is the usual one.

The typical synchrotron radiation frequency ν_m satisfies

$$\nu_m \propto \left(\frac{\Gamma}{\Gamma_o}\right)^{-5a/2} t^{-3/2} \propto t^{(15a-24)/16}, \tag{16}$$

where $\Gamma \approx 25\ E_{iso,53}^{1/8}\ [2/(1+z)]^{-3/8}\ t_{d,-1}^{-3/8}\ n_0^{-1/3}$.

The cooling frequency ν_c satisfies

$$\nu_c \propto \left(\frac{\Gamma}{\Gamma_o}\right)^{3a/2} t^{-1/2} \propto t^{-(8+9a)/16}. \tag{17}$$

The maximum spectral flux $F_{\nu,max}$ satisfies

$$F_{\nu,max} \propto \left(\frac{\Gamma}{\Gamma_o}\right)^{-a/2} \propto t^{3a/16}. \tag{18}$$

The observed flux behaves as (in this subsection, we take $a = 1$)

$$F_{\nu_X} \propto \begin{cases} F_{\nu,max}\nu_c^{-1/3} \propto t^{(4+9a)/24} \sim t^{0.55}, \\ \qquad\qquad \text{for } \nu_X < \nu_c < \nu_m; \\ F_{\nu,max}\nu_c^{1/2} \propto t^{-(8+3a)/32} \sim t^{-0.35}, \\ \qquad\qquad \text{for } \nu_c < \nu_X < \nu_m; \\ F_{\nu,max}\nu_m^{-1/3} \propto t^{(4-a)/8} \sim t^{0.38}, \\ \qquad\qquad \text{for } \nu_X < \nu_m < \nu_c; \\ F_{\nu,max}\nu_m^{(p-1)/2} \propto t^{(15ap-9a-24p+24)/32} \sim t^{-0.2}, \\ \qquad\qquad \text{for } \nu_m < \nu_X < \nu_c; \\ F_{\nu,max}\nu_c^{1/2}\nu_m^{(p-1)/2} \propto t^{(16-18a-24p+15ap)/32} \sim t^{-0.65}, \\ \qquad\qquad \text{for } \nu_X > \max\{\nu_c, \nu_m\}. \end{cases} \tag{19}$$

The afterglow light curves are shown in Fig. 4. As both ϵ_e and ϵ_B increase with time, the flux of the early X-ray emission is dimmer than that of the constant shock parameters model and the decline is much slower. Both are consistent with the current *Swift* XRT observations (Nousek et al. 2005).

3.4 A very low non-constant density

In the standard interstellar medium (ISM) afterglow model, the number density of the medium is taken as a constant. In the wind model, the number density n decreases with the radius R as $n \propto R^{-2}$ (Mészáros et al. 1998; Dai & Lu 1998b; Chevalier & Li 2000). Here we discuss the general case $n \propto R^{-k}$ ($0 \leqslant k < 3$).

First, we show that for a fireball decelerating in the Blandford–McKee self-similar regime (Blandford & McKee 1976), no X-ray flattening is expected regardless of the choice of k. The energy of the fireball is nearly constant and it is given by $E_{iso} \approx \Gamma^2\, Mc^2$, where $M \propto R^{3-k}$ is the total mass of the swept medium. So $\Gamma \propto R^{-(3-k)/2}$. Considering that $\mathrm{d}R \propto \Gamma^2\, \mathrm{d}t \propto R^{-(3-k)}\, \mathrm{d}t$, we have $R \propto t^{1/(4-k)}$ and $\Gamma \propto t^{-(3-k)/[2(4-k)]}$.

Now ν_m decreases with t as

$$\nu_m \propto \Gamma^4 R^{-k/2} \propto t^{-3/2}, \tag{20}$$

and ν_c and $F_{\nu,max}$ satisfy

$$\nu_c \propto \Gamma^{-4} R^{3k/2} t^{-2} \propto t^{(3k-4)/[2(4-k)]}, \tag{21}$$

$$F_{\nu,max} \propto R^{3-3k/2}\Gamma^2 \propto t^{-k/[2(4-k)]}, \tag{22}$$

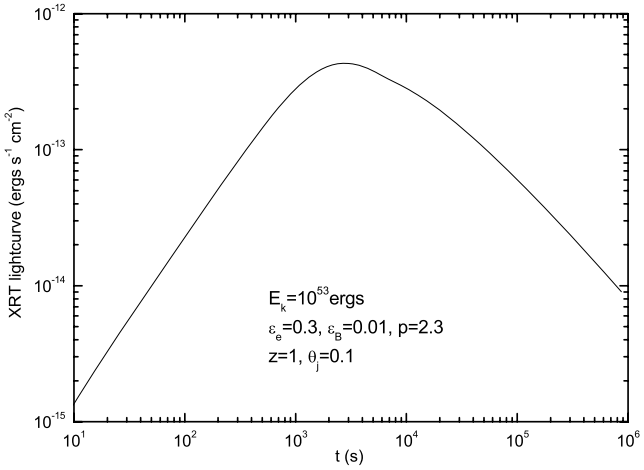

Figure 5. X-ray (0.2–10 keV) afterglow light curve for a very low non-constant density: $n = 10^{-4}\,\mathrm{cm}^{-3}$ for $R < 10^{16}$ cm; $n = 10^{-4}\,(R/10^{16})^{-1}\,\mathrm{cm}^{-3}$ for $10^{16} < R < 10^{19}$ cm and $n = 10^{-7}\,\mathrm{cm}^{-3}$ for $R > 10^{19}$ cm.

respectively. This results in

$$F_{\nu_X} \propto \begin{cases} t^{-3(p-1)/4-k/[2(4-k)]}, & \text{for } \nu_m < \nu_X < \nu_c; \\ t^{-1/4}, & \text{for } \nu_c < \nu_X < \nu_m; \\ t^{-(3p-2)/4}, & \text{for } \nu_X > \max\{\nu_m, \nu_c\}. \end{cases} \quad (23)$$

The last two are independent of k. So no X-ray flattening appears.

However, if the number density is sufficiently low, the deceleration time-scale ($\propto n^{-1/3}$) can be very long and even as long as $\sim 10^4$ s. In this case, a slowly decaying X-ray afterglow may be obtained. One example has been plotted in Fig. 5, in which the density profile of the medium is taken as $n = 10^{-4}\,\mathrm{cm}^{-3}$ for $R \leqslant 10^{16}$ cm, $n = 10^{-4}\,R_{16}^{-1}\,\mathrm{cm}^{-3}$ for $1 \leqslant R_{16} \leqslant 10^3$ and $n = 10^{-7}\,\mathrm{cm}^{-3}$ for $R_{16} > 10^3$. An X-ray flattening appears when the shock front reaches $R = 10^{19}$ cm. However, while the shape of the light curve is correct the X-ray flux is too low to account for most XRT light curves.

3.5 Magnetized outflow

A Poynting flux dominated outflow (Lyutikov & Blandford 2003; Thompson 1994; Usov 1994) is an alternative to the standard baryonic fireball model. Within the context of this discussion it is of interest since it may also give rise to a slowly decaying X-ray afterglow (Zhang et al. 2005). We investigate, here, briefly this possibility, extended discussion will be presented elsewhere.

We assume that the electromagnetic energy E_p will be transformed continuously into the kinetic energy of the forward shock. The dynamical evolution of the shocked medium is governed by (Huang et al. 2000; Wei et al. 2006)

$$\mathrm{d}\Gamma = -\frac{(\Gamma^2 - 1)\,\mathrm{d}m + \mathrm{d}E_p/c^2}{M_{\rm ej} + \epsilon m + 2(1-\epsilon)\Gamma m}, \quad (24)$$

where $E_p \equiv \Gamma^2 V B'^2/(4\pi)$, V is the volume of the magnetized outflow (measured by the observer) and B' is the comoving strength of the magnetic field.

If the magnetic pressure is higher than the thermal pressure of the shocked medium, the magnetic pressure works on the shocked medium and the kinetic energy of the forward shock increases. A pressure balance between the shocked medium and the magnetized outflow is established, so we have (see also Lyutikov & Blandford 2003) $B'^2/(8\pi) = p_{\rm gas} \simeq 4\Gamma^2\, nm_p c^2/3$, where $p_{\rm gas}$ is the thermal pressure of the shocked medium. Therefore, E_p can be estimated by[4]

$$E_p = 2\Gamma^2 P_{\rm gas} V \approx 8\Gamma^4 n m_p c^2 V/3. \quad (25)$$

$\mathrm{d}E_p/c^2$ can be calculated as follows. Assuming that the whole system (the shocked medium and the magnetized outflow) is adiabatic (i.e. the radiation efficiency $\epsilon = 0$), the energy conservation yields

$$2\Gamma^2 p_{\rm gas} V + 3\Gamma^2 p_{\rm gas}(V_{\rm tot} - V) = E_{\rm tot} - \Gamma(M_{\rm ej} + m)c^2, \quad (26)$$

where $V_{\rm tot} \approx 4\pi R^2 \Delta$ is the total volume of the system, Δ is the width of the system, which is described by $\mathrm{d}\Delta = (\beta_{\rm fsh} - \beta)\,\mathrm{d}R$ and $\beta_{\rm fsh} \simeq \sqrt{\Gamma^2 - 1}/[\Gamma - 1/(4\Gamma + 3)]$ is the velocity of the forward shock. Differentiating equation (26) we obtain

$$\mathrm{d}E_p/c^2 = 2\{(16\Gamma^3 n m_p V_{\rm tot} + M_{\rm ej} + m)\,\mathrm{d}\Gamma + 16\pi\Gamma^4 R n m_p \times [R(\beta_{\rm fsh} - \beta) + 2\Delta]\,\mathrm{d}R + \Gamma\,\mathrm{d}m\}. \quad (27)$$

After simple algebra, equation (24) can be rearranged as (note that now we take $\epsilon = 0$)

$$\mathrm{d}\Gamma = -\frac{(\Gamma^2 + 2A\Gamma - 1)\,\mathrm{d}m + B\,\mathrm{d}R}{M_{\rm ej} + 2\Gamma m + 2A(16\Gamma^3 n m_p V_{\rm tot} + M_{\rm ej} + m)}, \quad (28)$$

where $A = 1$ for $\mathrm{d}E_p/\mathrm{d}R \leqslant 0$, otherwise $A = 0$; $B = 32A\pi n m_p\,\Gamma^4 R\,[(\beta_{\rm fsh} - \beta)R + 2\Delta]$.

With proper boundary conditions and the relations $\mathrm{d}m = 4\pi n m_p R^2\,\mathrm{d}R$, $\mathrm{d}R = \beta c\Gamma^2(1+\beta)\,\mathrm{d}t/(1+z)$, $V_{\rm tot} = 4\pi R^2\Delta$ and $\mathrm{d}\Delta = (\beta_{\rm fsh} - \beta)\,\mathrm{d}R$, equation (28) can be solved numerically. In our numerical example, we take $E_k = 10^{52}$ erg, $n = 1\,\mathrm{cm}^{-3}$, $E_p = 10E_k$ and the width of the outflow is taken as 3×10^{11} cm. The starting point of our calculation is at $R = 2 \times 10^{16}$ cm ($\sim R_{\rm dec}$, the deceleration radius of the outflow, where $\sim E_k/2$ has been given to the shocked medium), at which $\Gamma = 360$.[5] We find out that most of the magnetic energy has been converted into the kinetic energy of the forward shock in a very short time $\sim 50(1+z)$ s. A similar result has been obtained by Lyutikov & Blandford (2003). Though this time-scale is much longer than the crossing time of the reverse shock, it is not long enough to account for the X-ray flattening detected in most GRBs.

4 CASE STUDIES: CONSTRAINING THE MODELS

GRB 050319 and GRB 050401, have well-recorded X-ray and optical afterglows, with which the models discussed in Section 3 can

[4] Providing that $V \propto R^{2+c}\,\Gamma^{-d}$, $E_p \propto \Gamma^{8+2c-d}\,t^{2+c} \propto t^{-\delta}$ (c, d and δ are all larger than 0), we have $\Gamma \propto t^{-(2+c+\delta)/(8+2c-d)}$, which should be flatter than $\Gamma^{-3/8}$ (the canonical dynamical evolution of a ejecta without energy injection). It requires that $2c + 3d < 8 - 8\delta$, otherwise $\mathrm{d}E_p/\mathrm{d}t < 0$ has been violated. It is evident that in the spreading phase, i.e. $c = 1$ and $d = 2$, E_p can not be converted into the kinetic energy of the forward shock effectively.

[5] At that radius, the reverse shock has crossed the ejecta and a pressure balance between the shocked medium and the magnetized outflow is reached. In this work, we do not calculate the reverse shock emission (see Fan, Wei & Wang 2004a) for the reverse shock emission with mild magnetization and Zhang & Kobayashi (2005) for reverse shock emission with arbitrary magnetization. With the ideal MHD jump condition, the reverse shock can not convert the magnetic energy into the kinetic energy of the forward shock effectively, as shown in Kennel & Coronitti (1984), Fan, Wei & Zhang (2004b) and Zhang & Kobayashi (2005) both analytically and numerically.

be constrained. We discuss these constraints in detail here. For most *Swift* GRBs only the X-ray afterglow is well detected. Such bursts provide, of course, much weaker constraints on the model. We discuss one example, GRB 050315, briefly.

4.1 GRB 050319

Both the optical and X-ray afterglows of GRB 050319 have been well recorded (Mason et al. 2006; Nousek et al. 2005; Woźniak et al. 2005; Cusumano et al. 2006). The optical flux declines with a power-law slope of $\alpha = -0.57$ between $\sim$200 s after the burst onset until it fades below the sensitivity threshold of the *UVOT* after 5 $\times$ 10^4 s. The optical V-band emission lies on the extension of the X-ray spectrum, with an spectral slope $\beta = -0.8$ (Mason et al. 2006). The temporal behaviour of the X-ray afterglow is more complicated. After a steep decay ($\alpha = -5.53$) up to $t = 370$ s, the light curve shows a slow decay with a temporal index of $\alpha = -0.54$. It steepens to $\alpha = -1.14$ at $t = 2.60 \times 10^4$ s. The spectral indices in the slow decline phase and the normal decay phase are $\beta = -0.7$ and $\beta = -0.8$, respectively (Cusumano et al. 2005; Nousek et al. 2005, However, see Quimby et al. 2006). Below we examine whether the models discussed above (in Section 3) can explain both the optical and the X-ray afterglows self-consistently.

Energy injection: The energy injection model is believed to able to explain the observation (e.g. Cusumano et al. 2005; Mason et al. 2006; Zhang et al. 2005). As shown in Section 3.1, for $q = 0.6$ and $p = 2.4$, both the optical and the X-ray afterglows decline as $F_{\nu_{\rm X}} \propto t^{-0.54}$ when $\nu_{\rm m} < \nu_R < \nu_{\rm X} < \nu_{\rm c}$, the corresponding spectral index should be $\beta = -(p-1)/2 \sim -0.7$. All these values are consistent with the observation. However, the non-detection of the further X-ray break caused by the spectral translation ($\nu_{\rm c} < \nu_{\rm X}$) up to $\sim 10^6$ s after the trigger suggests that $\epsilon_B \sim 5 \times 10^{-3}$ and $n \sim 10^{-3}\,{\rm cm}^{-3}$ (Cusumano et al. 2005). The problem is that $F_{\nu_{\rm X}}$ depends on n and ϵ_B sensitively for $\nu_{\rm X} < \nu_{\rm c}$ (see equation 7). The smaller n and ϵ_B, the smaller $F_{\nu_{\rm X}}$. We show below that it is quite difficult to reproduce the detected X-ray and optical light curves with the energy injection model.

The earliest R-band data is collected at $\sim$200 s (note that the real onset of GRB 050319 is about 130 s before the *Swift* trigger time taken in Woźniak et al. 2005, see Cusumano et al. 2005 for clarification), and the flux is about $F_{\nu_R} \sim 0.7$ mJy. At that time, the total energy of the outflow is still dominated by the initial E_k, and $F_{\nu,\rm max}$ and $\nu_{\rm m}$ are still described by equations (2) and (3), respectively. The conditions $F_{\nu,\rm max} \geqslant 0.7$ mJy and $\nu_{\rm m}(t \sim 200\,{\rm s}) \leqslant \nu_R$ yield

$$\epsilon_{B,-2}^{1/2} E_{k,53} n_0^{1/2} \geqslant 0.8 \Rightarrow E_{k,53} \geqslant 0.8 \epsilon_{B,-2}^{-1/2} n_0^{-1/2}, \quad (29)$$

$$E_{k,53}^{1/2} \epsilon_{B,-2}^{1/2} \epsilon_{\rm e,-1}^2 \leqslant 0.04 \Rightarrow \epsilon_{\rm e} \leqslant 0.02 E_{k,53}^{-1/4} \epsilon_{B,-2}^{-1/4}, \quad (30)$$

respectively. The condition $\nu_{\rm c} \geqslant \nu_{\rm X} \sim 10^{17}$ Hz holding up to $t \sim 10^6$ s gives

$$E_{k,53}^{-1/2} \epsilon_{B,-2}^{-3/2} n_0^{-1} (1+Y_{\rm o})^{-2} \geqslant 940$$
$$\Rightarrow \epsilon_B \leqslant 10^{-4} E_{k,53}^{-1/3} n_0^{-2/3} (1+Y_{\rm o})^{-4/3}, \quad (31)$$

where $Y_{\rm o}$ is the Compton parameter at $t \sim 10^6$ s. To derived this relation, we assume that at $t \sim 200$ s, $\nu_{\rm c}$ is described by equation (4), and $\nu_{\rm c} \propto t^{(q-2)/2} \sim t^{-0.7}$ up to $t \sim 2.6 \times 10^4$ s (i.e. in the energy injection phase), then $\nu_{\rm c} \propto t^{-1/2}$ up to $t \sim 10^6$ s.Combing equations (29–31), we have

$$E_{k,53} \geqslant 13 n_0^{-1/5} (1+Y_{\rm o})^{4/5}, \quad (32)$$

$$\epsilon_{\rm e} \leqslant 0.06 E_{k,53}^{-1/6} n_0^{1/6} (1+Y_{\rm o})^{1/3}. \quad (33)$$

Now $Y_0 \sim 0$ (see Appendices A and B for detail), we have $E_k > 1.3 \times 10^{54}\,{\rm erg}\, n_0^{-1/5}$. On the other hand, the energy injection coefficient $A' \equiv Ac^2 \sim (1+z) E_k / t_0 \sim 1.4 \times 10^{52}\, n_0^{-1/5}\,{\rm erg\,s^{-1}}$ for $t_0 \sim 370$ s. Please note that A' is comparable to the recorded luminosity of most GRBs and the X-ray luminosity recorded by XRT is just $\sim 10^{48}\,{\rm erg\,s^{-1}}$. The outflow accounting for the late-time injection is so energetic that strong soft X-ray to γ-ray emission powering by shocks or magnetic dissipation are expected. They will quite likely dominate over the corresponding forward shock emission, which is inconsistent with the observation.

This model is also disfavoured by the different temporal behaviour of the X-ray and the optical afterglows at $t > 2.6 \times 10^4$ s. We therefore conclude that the energy injection model cannot account for the multiwavelength afterglows of GRB 050319. We tried to fit both the R-band and X-ray afterglows with reasonable parameters numerically but failed.

Provided that the energy injection model works (i.e. there is a mechanism to keep such energetic outflow steady enough and there is no magnetic dissipation), the initial GRB efficiency in this case is as low as $\tilde{\epsilon}_\gamma = E_\gamma/(E_\gamma + E_k) \sim 0.08 n_0^{1/5}$.

Small $\zeta_{\rm e}$: This model is disfavoured by two facts. One is that in the X-ray flattening phase, $\nu_{\rm c} < \nu_{\rm X} < \nu_{\rm m}$, the corresponding spectral index is $\beta \sim -1/2$, which only marginally matches the observation ~ -0.7. The other is that after the temporal transition at $t \sim 10^4$ s, $\nu_{\rm c} < \nu_{\rm m} < \nu_{\rm X}$, the spectral index should be $\beta = -p/2 \sim -1.2$, which is inconsistent with the observation.

Evolving shock parameters: As shown in Section 3.3, for $\nu_{\rm m} < \nu_R < \nu_{\rm X} < \nu_{\rm c}$, $p = 2.4$ and $a = b = 0.6$, $(F_{\nu_R}, F_{\nu_{\rm X}}) \propto t^{-0.54}$ and the spectral index $\beta = -(p-1)/2 \sim -0.7$, are all consistent with the observation. After the shock parameters saturate at $t \sim 2.6 \times 10^4$ s, $F_{\nu_{\rm X}} \propto t^{-1.1}$ and $\beta = -0.7$ as long as $\nu_{\rm X} < \nu_{\rm c}$, which also matches the observation. However, the optical light curve should be much steeper since $\nu_{\rm m} < \nu_R < \nu_{\rm c}$ also holds. The *UVOT* observation and the ground based$R$-band observation suggest that the decline of optical emission does not change up to $t \sim 2 \times 10^5$ s, though the scatter of the flux is quite large (Kiziloglu et al. 2005; Sharapov et al. 2005; see Mason et al. 2006 for a summary). Therefore the evolving shock parameter model is disfavoured.

Very low non-constant density: With proper parameters as well as proper density profile, an X-ray flattening does appear (see Fig. 5). However, as already mentioned, the flux is too low to match most observations, here we do not discuss it further.

Off-beam annular jet model: Recently, Eichler & Granot (2006) suggested that the flat part of the XRT light curve may be a combination of the decaying tail of the prompt γ-ray emission and the delayed onset of the afterglow emission observed from viewing angles slightly outside of the edge of the jet (i.e. off-beam). This model, like others mentioned above, can account for the slow decline of many X-ray afterglows, but may be unable to explain both the optical and the X-ray afterglows of GRB 050319 self-consistently, as shown below.

Following Eichler & Granot (2006), we assume that the off-beam angle is $\delta\theta \sim 1/\Gamma_{\rm int}$, where $\Gamma_{\rm int}$ is the initial Lorentz factor of the outflow. Larger $\delta\theta$ is less favoured since the slowly decaying R-band afterglow has been well recorded as early as $t \sim 200$ s, which implies that the afterglow onset has not been delayed so much. In the off-beam case, the typical synchrotron radiation frequency should be

$$\nu_{\rm m} \approx 7.6 \times 10^{11}\,{\rm Hz}\, E_{k,53}^{1/2} \epsilon_{B,-2}^{1/2} \epsilon_{\rm e,-1}^2 C_p^2 \left(\frac{1+z}{2}\right)^{1/2} a^{1/2} t_{\rm d}^{-3/2}, \quad (34)$$

where $a \approx [1 + (\Gamma_{\rm int}\,\delta\theta)^2] \sim 2$ is the Doppler factor. Therefore, the condition $\nu_{\rm m}(t \sim 200\,{\rm s}) < \nu_R$ results in

$$\epsilon_{\rm e} \leqslant 0.017 E_{k,53}^{-1/4} \epsilon_{B,-2}^{-1/4} (a/2)^{-1/4}. \quad (35)$$

For $\delta\theta \sim 1/\Gamma_{\rm int}$, the late-time (i.e. the normal decline phase) afterglow emission is quite similar to the on-beam case (Eichler & Granot 2006).

We use equation (7) to estimate the late-time X-ray flux, though the predicted flux of the annular jet model should be somewhat different from that of our conical jet model (Eichler & Granot 2006; Granot 2005). The XRT flux $\approx 8 \times 10^{-12}\,{\rm erg\,s^{-1}\,cm^{-2}}$ at $t_{\rm d} \sim 0.3$ gives

$$E_{k,53} \approx 0.33 \epsilon_{\rm e,-1}^{4(1-p)/(p+3)} \epsilon_{B,-2}^{-(p+1)/(p+3)} n_0^{-2/(p+3)}. \quad (36)$$

The condition $\nu_{\rm c} > \nu_{\rm X} \sim 10^{17}$ Hz holding up to $t \sim 10^6$ s yields

$$\epsilon_B < 3 \times 10^{-4} E_{k,53}^{-1/3} n_0^{-2/3}. \quad (37)$$

Combing equations (35–37), we have $E_k > 10^{55}\,{\rm erg}\, n_0^{-1/5} (a/2)^{3(p-1)/10}$. While we manage to fit both X-ray and optical data, the energy needed is too large for any realistic progenitor models. We therefore suggest that the off-beam annular jet model is also unable to account for the afterglows of GRB 050319.

4.2 GRB 050401

The early X-ray light curve is consistent with a broken power law with $\alpha = -0.63$ and -1.41 respectively, the break is at $t_b \sim 4480$ s (de Pasquale et al. 2006). The X-ray spectral indices before and after the break are nearly constant ~ -0.90. Therefore, the small $\zeta_{\rm e}$ model is ruled out directly. Zhang et al. (2005) also show that the flat electron distribution model ($1 < p < 2$) is unable to account for the X-ray afterglow observation. The afterglow has also been detected in *R*-band, which decays as a simple power law $\propto t^{-0.76}$ up to $t \sim 3.5 \times 10^4$ s (Rykoff et al. 2005).

Energy injection ($p \sim 2.8$)**:** After the break, the light curve is consistent with an ISM model for $\nu_{\rm m} < \nu_{\rm X} < \nu_{\rm c}$ with $p \sim 2.8$. Before the break, it is consistent with the same model with $q = 0.5$ (see also Zhang et al. 2005). As far as the *R*-band afterglow emission is concerned, there are two possibilities. One is that $\nu_{\rm m} < \nu_R < \nu_{\rm c}$, the optical afterglow should follow the temporal behaviour of the X-ray afterglow, which is not the case. The other is that $\nu_R < \nu_{\rm m}$ for $t \leqslant t_b$, the afterglow increases as $t^{0.9}$ for $q \sim 0.5$ (see Section 3.1), which is inconsistent with the observation. We therefore conclude that the popular energy injection model is unable to account for the data in this burst as well.

Evolving shock parameters ($p \sim 2.8$)**:** The light curve after the break is consistent with an ISM model for $\nu_{\rm m} < \nu_{\rm X} < \nu_{\rm c}$ with $p \sim 2.8$. Before the break, it is consistent with the same model with $a = b = 0.7$. Can it reproduce the optical afterglow? The answer is negative. Provided that $\nu_R < \nu_{\rm m}$ for $t \leqslant t_b$, the optical afterglow should increase as $t^{0.4}$ (see Section 3.3), which is inconsistent with the data. The case of $\nu_{\rm m} < \nu_R$ is ruled out directly in view of the different temporal behaviour of X-ray and *R*-band afterglows.

4.3 GRB 050315

After a steep decay up to $t_{b1} = 308$ s, the X-ray light curve shows a flat 'plateau' with a temporal index of $\alpha = -0.06$ (the spectral index of XRT data is $\beta = -0.73$). It then turns to $\alpha = -0.71$ at $t_{b2} = 1.2 \times 10^4$ s, the spectral index is $\beta = -0.79$. Finally, there is a third break at $t_{b3} = 2.5 \times 10^5$ s, after which the temporal decay index is $\alpha = -2.0$ and the spectral index is $\beta = -0.7$ (Barthelmy et al. 2005; Nousek et al. 2005).

There are two possible interpretations for the long-term constant spectral index $\beta \sim -0.7$. One is that $\max\{\nu_{\rm c}, \nu_{\rm m}\} < \nu_{\rm X}$ after $t = 308$ s and the power-law index of the shocked electron $p \sim 1.5$. The other is that $\nu_{\rm m} < \nu_{\rm X} < \nu_{\rm c}$ for $t_{b1} < t < t_{b3}$ and $p \sim 2.5$.

Energy injection ($p \sim 2.5$)**:** To obtain the slow decline for $t_{b1} < t < t_{b2}$, energy injection with $q \sim 0.2$ is needed. $q \sim 0.9$ is needed to reproduce the X-ray afterglows at $t_{b2} < t < t_{b3}$. The late-time sharp decay appears when the boundary of a non-spreading jet becomes visible.

Evolving shock parameters ($p \sim 2.5$)**:** As shown in Section 3.3, with $a = b = 1.2$, we have a slow decline slope $\alpha = -0.06$ between t_{b1} and t_{b2}. To get a decline slope $\alpha = -0.71$ between t_{b2} and t_{b3}, $a = b = 0.45$ are needed. The late-time sharp decay appears when the boundary of a non-spreading jet becomes visible and $a = b = 0.45$.

We find that both models can explain the observed X-ray light curves of GRB 050315.

5 SUMMARY AND DISCUSSION

During the past several months, the *Swift* XRT has collected a rich sample of early X-ray afterglow data. A good fraction of these afterglows show a slow decline phase lasting between a few hundred to several thousand seconds. The energy injection model is the leading model to account for these slowly decaying X-ray afterglows (e.g. Nousek et al. 2005; Zhang et al. 2005; Granot & Kumar 2006; Panaitescu et al. 2006). It has been suggested that in this model, the GRB efficiency might be as high as 90 per cent. Such a high-efficiency challenges the standard internal shock model for the prompt γ-ray emission.

In this work, we have re-examined the GRB efficiency of several pre-*Swift* GRBs and one *Swift* GRB. In addition, we have explored several mechanism which might give rise to a slowly decaying X-ray light curve and we have compared the predictions of these models with the well-recorded multiwavelength afterglows of GRB 050319 and GRB 050401. We draw the following conclusions:

(1) The GRB efficiency of pre-*Swift* GRBs that has been derived directly from the X-ray flux 10 h after the burst has been overestimated. For these *Swift* GRBs with long-time X-ray flattening, the GRB efficiency is also moderate (around 0.5), even when taking into account the possibility of energy injection. Such efficiency can be understood within the standard internal shock model.

(2) With a proper choice of parameters, the slow decline slope of X-ray afterglow like the one detected in GRB 050319 can be well reproduced by several models – the energy injection model, evolving shock parameter model (in which the shock parameters are assumed to increase with the decrease of the shock strength for $t < 10^4$ s), the small $\zeta_{\rm e}$ model (in which the shock energy has been give to a fraction $\zeta_{\rm e}$ of electrons, rather than total) and the very low non-constant density model. Out of these models, the last two are ruled out by the X-ray data itself. In the last model, the resulting X-ray afterglow is too dim to match most XRT observations. The small $\zeta_{\rm e}$ model is also disfavoured since (1) in the slow decline phase, the XRT spectrum are usually much softer than $\nu^{-1/2}$; (2) after the light-curve break, no spectral steepening has been detected in most cases, which is inconsistent with the model. The other models, including the energy injection model and the evolving shock parameter model seem to be consistent with the X-ray afterglow observations.

(3) While two models, the energy injection model and the evolving shock parameter model, are consistent with the X-ray data, they fail to reproduce both the X-ray and the optical afterglows of GRB 050319 and GRB 050401. In each burst, the optical flux declines slowly up to $\sim 10^5$ s. On the other hand, the X-ray light curve decays slowly up to $t \sim 10^4$ and then turns to the normal faster decay ($F \propto t^{-1.2}$ or so). The temporal index of the slow decay X-ray phase is close to that of the optical light curve. The XRT spectrum is unchanged before and after the X-ray break. This means that the break is not caused by a cooling break in which ν_c crosses the observed frequency.

The failure of all models that we considered to fit both the X-ray and the optical afterglow light curves suggests that we should look for another alternative. An intriguing possibility is based on fact that the extrapolation backwards of the late X-ray light curve is in agreement with (or 1–2 order lower than) the prompt X-ray emission. This suggests that we face a 'missing energy problem'. Namely, during the slow decay phase (in which the X-ray flux is rather low) we miss X-ray emission. Is it possible that during this phase this energy is dissipated into a different channel and not into synchrotron X-rays and that this different channel becomes ineffective at around 10 h? Put differently, during this phase the electrons within the forward shock emit synchrotron X-rays inefficiently. A possibility of this kind (that we have considered and found not to work) is if the X-ray emitting electrons are cooled efficiently via inverse Compton (and hence their synchrotron X-ray emission is weaker). As already mentioned inverse Compton cooling is important in determining the X-ray flux. Furthermore, due to the Klein–Nishina cut-off this cooling becomes unimportant at approximately 1 d. However, this transition is not sharp enough to produce the observed slowly decaying X-ray light curves. While inverse Compton cooling does not work it is possible that another, yet unexplored, process of this kind is responsible for the observed light curves.

ACKNOWLEDGMENTS

We thank A. Panaitescu and E. Waxman for their constructive comments. We also thank the referee for helpful suggestion. YF thanks D. M. Wei for his help and J. Dyks for checking Fig. 5. This work is supported by US-Israel BSF. TP acknowledges the support of Schwartzmann University Chair. YF is also supported by the National Natural Science Foundation (grants 10225314 and 10233010) of China, and the National 973 Project on Fundamental Researches of China (NKBRSF G19990754).

REFERENCES

Akerlof C. et al., 1999, Nat, 398, 400
Barthelmy S. D. et al., 2005, ApJ, 635, L133
Blandford R. D., McKee C. F., 1976, Phys. Fluids, 19, 1130
Beloborodov A. M., 2000, ApJ, 539, L25
Berger E., Kulkarni S. R., Frail D. A., 2004, ApJ, 612, 966
Blustin A. J. et al., 2006, ApJ, 637, 901
Campana S. et al., 2005, ApJ, 625, L23
Chevalier R. A., Li Z. Y., 2000, ApJ, 536, 195
Cusumano G. et al., 2006, ApJ, 639, 316
Dai Z. G., 2004, ApJ, 606, 1000
Dai Z. G., Lu T., 1998a, A&A, 333, L87
Dai Z. G., Lu T., 1998b, MNRAS, 298, 87
Daigne F., Mochkovitch R., 1998, MNRAS, 296, 275
de Pasquale M. et al., 2006, MNRAS, 365, 1031
Dyks J., Zhang B., Fan Y. Z. 2005, ApJ, submitted, preprint (astro-ph/0511699)
Eichler D., Granot J. 2006, ApJ, 641, L5
Fan Y. Z., Dai Z. G., Huang Y. F., Lu T., 2002, Chin. J. Astron. Astrophys., 2, 449, preprint (astro-ph/0306024)
Fan Y. Z., Wei D. M., Wang C. F., 2004a, A&A, 424, 477
Fan Y. Z., Wei D. M., Zhang B., 2004b, MNRAS, 354, 1031
Fan Y. Z., Zhang B., Proga D., 2005a, ApJ, 635, L129
Fan Y. Z., Zhang B., Wei D. M., 2005b, ApJ, 628, L25
Freedman D. L., Waxman E., 2001, ApJ, 547, 922
Granot J., 2005, ApJ, 631, 1022
Granot J., Kumar P., 2006, MNRAS, 366, L13
Granot J., Piran T., Sari R., 1999, ApJ, 513, 679
Granot J., Nakar E., Piran T., 2003, Nat, 426, 138
Granot J., Königl A., Piran T. 2006, MNRAS, submitted, preprint (astro-ph/0601056)
Huang Y. F., Gou L. J., Dai Z. G., Lu T., 2000, ApJ, 543, 90
Ioka K., Toma K., Yamazaki R., Nakamura T. 2005, A&A, submitted, preprint (astro-ph/0511749)
Kennel C. F., Coronitti E. V., 1984, ApJ, 283, 694
Kiziloglu U. et al., 2005, GCN Circ., 3139
Kobayashi S., Sari R., 2001, ApJ, 551, 943
Kobayashi S., Piran T., Sari R., 1997, ApJ, 490, 92
Kumar P., 2000, ApJ, 538, L125
Kumar P., Panaitescu A., 2003, MNRAS, 346, 905
Kumar P., Piran T., 2000, ApJ, 532, 286
Llod-Ronning N. M., Zhang B., 2004, ApJ, 613, 477 (LZ04)
Lyutikov M., Blandford R., 2003, preprint (astro-ph/0312347)
Mason K. O. et al., 2006, ApJ, 639, 361
McMahon E., Kumar P., Panaitescu A., 2004, MNRAS, 354, 915
Mészáros P., Rees M. J., Wijers R. A. M. J., 1998, ApJ, 499, 301
Moderski R., Sikora M., Bulik T., 2000, ApJ, 529, 151
Nousek J. A. et al., 2005, ApJ, in press, preprint (astro-ph/0508332)
Paczynski B., Xu G. H., 1994, ApJ, 427, 708
Panaitescu A., Kumar P., 2002, ApJ, 571, 779
Panaitescu A., Kumar P., 2004, MNRAS, 353, 511
Panaitescu A., Mészáros P., Rees M. J., 1998, ApJ, 503, 314
Panaitescu A., Mészáros P., Gehrels N., Burrows D., Nousek J., 2006, MNRAS, 366, 1357
Papathanassiou H., Mészáros P., 1996, ApJ, 471, L91
Piran T., 1999, Phys. Rep., 314, 575
Quimby R. M. et al., 2006, ApJ, 638, 920
Rees M. J., Mészáros P., 1994, ApJ, 430, L93
Rees M. J., Mészáros P., 1998, ApJ, 496, L1
Rykoff E. S. et al., 2005, ApJ, 631, L121
Sari R., 1997, ApJ, 497, L17
Sari R., Mészáros P., 2000, ApJ, 535, L33
Sari R., Piran T., 1997a, MNRAS, 287, 110
Sari R., Piran T., 1997b, ApJ, 485, 270
Sari R., Narayan R., Piran T., 1996, ApJ, 473, 204
Sari R., Piran T., Narayan R., 1998, ApJ, 497, L17
Sharapov D., Ibrahimov M., Karimov R., Kahharov B., Pozanenko A., Rumyantsev V., Beskin G., 2005, GCN Circ., 3140
Thompson C., 1994, MNRAS, 270, 480
Usov V. V., 1994, MNRAS, 267, 1035
Vaughan S. et al., 2006, ApJ, 638, 920
Wei D. M., Lu T., 1998, ApJ, 505, 252
Wei D. M., Lu T., 2000, A&A, 360, L13
Wei D. M., Yan T., Fan Y. Z., 2006, ApJ, 636, L29
Wijers R. A. M. J., Galama T. J., 1999, ApJ, 523, 177
Woźniak P. R., Vestrand W. T., Wern J. A., White R. R., Evans, S. M., Casperson D., 2005, ApJ, 627, L13
Yost S., Harrison F. A., Sari R., Frail D. A., 2003, ApJ, 597, 459
Zhang B., Kobayashi S., 2005, ApJ, 628, 315
Zhang B., Mészáros P., 2001, ApJ, 552, L35
Zhang B., Mészáros P., 2002, ApJ, 566, 712
Zhang B., Kobayashi S., Mészáros P., 2003, ApJ, 595, 950
Zhang B., Fan Y. Z., Dyks J., Kobayashi S., Mészáros P., Burrows D. N., Nousek J. A., Gehrels N., 2005, ApJ, in press preprint (astro-p/0508321)

APPENDIX A: THE GENERAL FORM OF THE INVERSE COMPTON PARAMETER

For the photons with frequency higher than $\hat{\nu}$, the Compton parameter should be suppressed significantly since it is the Klein–Nishina regime, where $\hat{\nu}$ is governed by $(1+z)\gamma_e h\hat{\nu} \sim \Gamma m_e c^2$, i.e.

$$\hat{\nu} \sim 1.2\times10^{20}\,\mathrm{Hz}\,(1+z)^{-1}\Gamma\gamma_e^{-1}. \tag{A1}$$

We extend the derivation of the Compton parameter Y given by Sari et al. (1996) to the general form, in the limit of single scattering. The ratio of the inverse Compton power ($P_{\rm IC}$) to the synchrotron power ($P_{\rm syn}$) of an electron with random Lorentz factor $\gamma_{\rm e}$ is given by

$$Y(\gamma_e) = \frac{P_{\rm IC}}{P_{\rm syn}} = \frac{\eta_{\rm KN}U_{\rm syn}}{U_B} = \frac{\eta\eta_{\rm KN}\epsilon_e}{[1+Y(\gamma_e)]\epsilon_B}, \tag{A2}$$

where $\eta_{\rm KN}$ is the fraction of synchrotron radiation energy of total electrons emitted at frequencies below $\hat{\nu}$. So we have

$$Y(\gamma_e) = (-1+\sqrt{1+4\eta\eta_{\rm KN}\epsilon_e/\epsilon_B})/2. \tag{A3}$$

Below we estimate the parameter $\eta_{\rm KN}$ in different cooling regimes.

A1 Slow cooling

$$F_\nu = F_0\begin{cases}(\nu/\nu_c)^{-(p-1)/2}, & \text{for } \nu_m<\nu<\nu_c;\\ (\nu/\nu_c)^{-p/2}, & \text{for } \nu_c<\nu<\nu_M.\end{cases} \tag{A4}$$

where $\nu_M \sim 2.8\times10^{22}\ \Gamma/(1+z)\,$Hz is the maximal synchrotron radiation frequency of the electrons accelerated by the forward shock. For $p>2$, the total energy emitted is $\int F_\nu d\nu = \frac{2F_0}{(3-p)}\nu_c^{(p-1)/2}[\frac{1}{(p-2)}\nu_c^{(3-p)/2}-\nu_m^{(3-p)/2}]$, where the photons with frequencies below ν_m have been ignored. Throughout the appendix, ν_c is still described by equation (4) but without the correction of $1/(1+Y)^2$. We have

$$\eta_{\rm KN}\sim\begin{cases}0, & \text{for } \hat{\nu}<\nu_m;\\ \frac{\hat{\nu}^{(3-p)/2}-\nu_m^{(3-p)/2}}{[1/(p-2)]\nu_c^{(3-p)/2}-\nu_m^{(3-p)/2}}, & \text{for } \nu_m<\hat{\nu}<\nu_c;\\ 1-\frac{(3-p)\nu_c^{1/2}\hat{\nu}^{(2-p)/2}}{\nu_c^{(3-p)/2}-(p-2)\nu_m^{(3-p)/2}}, & \text{for } \nu_c<\hat{\nu}.\end{cases} \tag{A5}$$

For $1<p<2$, the total energy emitted is $\int F_\nu d\nu = \frac{2F_0}{(2-p)(3-p)}\nu_c^{(p-1)/2}S_1$, where $S_1 = [(3-p)\nu_c^{1/2}\ \nu_M^{(2-p)/2} - \nu_c^{(3-p)/2} - (2-p)\ \nu_m^{(3-p)/2}]$. Now $\eta_{\rm KN}$ can be estimated as

$$\eta_{\rm KN}\sim\begin{cases}0, & \text{for } \hat{\nu}<\nu_m;\\ \frac{(2-p)(\hat{\nu}^{(3-p)/2}-\nu_m^{(3-p)/2})}{S_1}, & \text{for } \nu_m<\hat{\nu}<\nu_c;\\ 1-\frac{(3-p)\nu_c^{1/2}(\nu_M^{(2-p)/2}-\hat{\nu}^{(2-p)/2})}{S_1}, & \text{for } \nu_c<\hat{\nu}<\nu_M.\end{cases} \tag{A6}$$

A2 Fast cooling

$$F_\nu = F_0\begin{cases}(\nu/\nu_m)^{-1/2}, & \text{for } \nu_c<\nu<\nu_m;\\ (\nu/\nu_m)^{-p/2}, & \text{for } \nu_m<\nu<\nu_M.\end{cases} \tag{A7}$$

For $p>2$, the total energy emitted is $\int F_\nu d\nu = 2F_0\nu_m^{1/2}[(\frac{p-1}{p-2})\nu_m^{1/2}-\nu_c^{1/2}]$, where the emission below ν_c has been ignored. The $\eta_{\rm KN}$ is estimated as

$$\eta_{\rm KN}\sim\begin{cases}0, & \text{for } \hat{\nu}<\nu_c;\\ \frac{\hat{\nu}^{1/2}-\nu_c^{1/2}}{[(p-1)/(p-2)]\nu_m^{1/2}-\nu_c^{1/2}}, & \text{for } \nu_c<\hat{\nu}<\nu_m;\\ 1-\frac{\nu_m^{(p-1)/2}\hat{\nu}^{(2-p)/2}}{(p-1)\nu_m^{1/2}-(p-2)\nu_c^{1/2}}, & \text{for } \nu_m<\hat{\nu}.\end{cases} \tag{A8}$$

For $1<p<2$, the total energy emitted is $\int F_\nu d\nu = \frac{2F_0\nu_m^{1/2}}{2-p}S_2$, where $S_2 = [\nu_m^{(p-1)/2}\ \nu_M^{(2-p)/2} - (p-1)\ \nu_m^{1/2} - (2-p)\nu_c^{1/2}]$. We have

$$\eta_{\rm KN}\sim\begin{cases}0, & \text{for } \hat{\nu}<\nu_c;\\ \frac{(2-p)(\hat{\nu}^{1/2}-\nu_c^{1/2})}{S_2}, & \text{for } \nu_c<\hat{\nu}<\nu_m;\\ 1-\frac{\nu_m^{(p-1)/2}[\nu_M^{(2-p)/2}-\hat{\nu}^{(2-p)/2}]}{S_2}, & \text{for } \nu_m<\hat{\nu}<\nu_M.\end{cases} \tag{A9}$$

APPENDIX B: WHEN IS THE KLEIN–NISHINA CORRECTION IMPORTANT?

In the shock front, the magnetic field strength B is

$$B = 0.04\Gamma\epsilon_{B,-2}^{1/2}n_0^{1/2}. \tag{B1}$$

The typical synchrotron radiation frequency of an electron with random Lorentz factor $\gamma_{\rm e}$ is

$$\nu(\gamma_e) = \frac{2.8\times10^6}{1+z}\ \mathrm{Hz}\ \gamma_e^2\Gamma B. \tag{B2}$$

B1 The XRT light curve

For $\nu_X\sim10^{17}$ Hz, we have $\gamma_e(\nu_X) = 1.3\times10^5[2/(1+z)]^{-1/2}\ \Gamma_1^{-1}\ \epsilon_{B,-2}^{-1/4}\ n_0^{-1/4}$ and

$$\hat{\nu}\sim5\times10^{15}\ \mathrm{Hz}\ [(1+z)/2]^{1/2}\Gamma_1^2\epsilon_{B,-2}^{1/4}n_0^{1/4}. \tag{B3}$$

Therefore, the Klein–Nishina correction seems to be unimportant (i.e. $\eta_{\rm KN}\sim1$) for $t_{\rm d}\sim1$ (when $\hat{\nu}\sim\nu_c$) and $\epsilon_B\sim0.01$.

B2 The *R*-band light curve

For $\nu_R\sim4.3\times10^{14}$ Hz, we have $\gamma_e(\nu_R) = 8\times10^3[2/(1+z)]^{-1/2}\ \Gamma_1^{-1}\ \epsilon_{B,-2}^{-1/4}\ n_0^{-1/4}$ and

$$\hat{\nu}\sim8\times10^{16}\ \mathrm{Hz}\ [(1+z)/2]^{1/2}\Gamma_1^2\epsilon_{B,-2}^{1/4}n_0^{1/4}. \tag{B4}$$

Then, with $\epsilon_B\sim0.01$, the Klein–Nishina correction seems to be unimportant for a long time. On the other hand, the factor $\eta\simeq\min\{1,(\nu_m/\nu_c)^{(p-1)/2}\}\sim1$ for $t_{\rm d}<1$. As a consequence, the inverse Compton effect is very important both for the long wavelength afterglow calculation and for the X-ray light-curve calculation. However, it may be unimportant for a lower ϵ_B since $\nu_c\propto\epsilon_B^{-3/2}$.

This paper has been typeset from a TEX/LATEX file prepared by the author.